ADVANCED ENGINEERING MATERIALS
www.aem-journal.com

Ultrafast Fabrication of Thermoelectric Films by Pulsed Light Sintering of Colloidal Nanoparticles on Flexible and Rigid Substrates

Roozbeh Danaei, Tony Varghese, Mostafa Ahmadzadeh, John McCloy, Courtney Hollar, Mohammad Sadeq Saleh, Jonghyun Park, Yanliang Zhang, and Rahul Panat**

Sintered thermoelectric (TE) nanoparticle films are known to have a high figure-of-merit ZT factor and are considered for waste hear recovery and heating and cooling applications. The conventional process of thermal sintering of TE nanoparticles requires an inert environment and long heating times, and cannot be used on polymer substrates due to the requirements of the process (e.g., heating up to 400 °C). In this communication, the authors demonstrate for the first time the use of an intense flash of UV light from a Xenon lamp to sinter TE nanoparticles within milliseconds under ambient conditions on flexible polymer as well as glass substrates to create functional TE films. Photonic sintering is used to fabricate Bismuth Telluride thermoelectric films with a conductivity of 3200 S m^{-1} (a 5–6 orders of magnitude increase over unsintered films) and a peak power factor of 30 μW m^{-1} K^{-2}. Modeling is used to gain an insight into the physical processes occurring during photonic sintering process and identify the critical parameters controlling the process. This work opens-up an exciting possibility of extremely rapid fabrication of TE generators under ambient conditions on a variety of flexible and rigid substrates.

Thermoelectric generators based on the Seebeck effect have shown a great promise for waste heat recovery in diverse applications such as automotive engines, power plants, and microelectronics.[1] Thermoelectric devices have also been considered for heating and cooling applications.[2] The efficiency of thermoelectric materials is determined by the figure-of-merit ZT which is defined by $ZT = \alpha^2 \sigma T/\kappa$, where α, σ, κ, and T are Seebeck coefficient, electrical conductivity, thermal conductivity, and absolute temperature, respectively. The ZT factor of TE generators can be significantly enhanced by making nanostructured TE materials using nanoparticles due to the reduction in lattice thermal conductivity.[3] High performance TE films have been demonstrated by printing nanoparticles followed by thermal sintering at around 400 °C in an inert environment.[4] However, the conventional sintering methods such as thermal sintering in a furnace suffer from two major limitations. First, the process of thermal sintering can take several hours per batch and is unsuitable for rapid fabrication methods such as roll-to-roll manufacturing[5] of TE generators. Second, the conventional thermal sintering exposes both the printed film and substrate to high temperatures, which limits the type of substrate that can be used to form the films.

To overcome these challenges, we demonstrate in this work the use of photonic sintering method[6,7] to create TE films from Bismuth Telluride-based nanoparticles where sintering/densification is achieved over large areas (several square inches), in extremely short periods of time (milliseconds per pulse) and using a rigid glass as well as flexible polymer substrate. Due to the high speed of sintering, this method is highly compatible with rapid roll-to-roll manufacturing of low-cost

Prof. Y. L. Zhang
Department of Aerospace and Mechanical Engineering
University of Notre Dame
Notre Dame, IN 46556, USA
E-mail: yzhang45@nd.edu

Prof. R. Panat, M. S. Saleh
Department of Mechanical Engineering
Carnegie Mellon University
Pittsburgh, PA 15213, USA rpanat@andrew.cmu.edu

R. Danaei, M. Ahmadzadeh, Prof. J. McCloy
School of Mechanical and Materials Engineering
Washington State University
Pullman, WA 99164, USA

T. Varghese
Micron School of Material Science and Engineering
Boise State University
Boise, ID 83725, USA

C. Hollar
Department of Mechanical Engineering
University of Idaho
Moscow, ID 83844, USA

Prof. J. H. Park
Department of Mechanical and Aerospace Engineering
Missouri University of Science and Technology
Rolla, MO 65409, USA

DOI: 10.1002/adem.201800800

printed TE generators for applications such as energy harvesting. We note that printed Bi_2Te_3 films have been used in the past as thermoelectric materials.[8] However, to the best of our knowledge, the photonic sintering of BiTe-based TE nanoparticles has not been demonstrated to date despite the progress in realizing TE devices using conventional thermal sintering.

We used $Bi_2Te_{2.8}Se_{0.2}$ nanoparticles synthesized using a microwave stimulated wet-chemical method described elsewhere.[3] A Xenon lamp was used for the photonic sintering of the TE nanoparticles. **Figure 1** shows the schematic of the process to make the TE films. The process consisted of creating and dispensing nanoparticle ink dispersion followed by thermal drying. The dried sample was cold pressed, followed by the exposure to xenon lamp flash. Scanning electron microscope images of the powder after thermal drying and after the photonic sintering, as well as an image of a flexible film on Kapton substrate are also shown in Figure 1. Details of the process to form the TE film are given in Experimental section. Note that the films were produced at different pulse durations and power densities using a single pulse of light on glass and Kapton substrates (see **Table 1**). Note that the sintering conditions used in this study were optimized for the current set of materials.

Figure 2a–d show the thermoelectric properties of the TE films. Figure 2a gives the film conductivity as a function of the pulse duration for films on glass substrate. The film conductivity increases dramatically from a low value (about 10^{-3} S m^{-1} for compacted but unsintered film) to 3.2×10^3 S m^{-1} upon exposure to photonic pulse duration of 2 ms (see Table 1 for power densities). This clearly indicates a sintering effect as observed qualitatively in the SEM images of Figure 1. The error bars represent a standard deviation for measurements of four samples. The electrical conductivity should eventually reach a plateau with further increases of pulsed length, which is not observed here due to the limit of the pulse length of our photonic machine. The room-temperature conductivity of the film on Kapton tape is about 1900 S m^{-1}, which is lower than the film on glass due to the lower power density applied on films on Kapton (Table 1). Note that for higher power densities on Kapton tape, film cracking was observed likely due to its higher thermal expansion coefficient compared to the glass substrates. The temperature dependent electrical conductivity of the films was also measured for single pulse sintered samples on glass (#S-2-1.37), and single pulse sintered sample on Kapton (#SK-1.5–0.9) and shown in Figure 2b. Figure 2c shows the temperature dependent Seebeck coefficients of samples in Figure 2a. Figure 2d shows the power factor ($\sigma\alpha^2$) as a function of temperature for the films. The sample sintered by the highest energy (#S-2-1.37) shows the highest power factor of about 30 μW m^{-1} K^{-2} at 200 °C. The power factor of our not yet fully optimized samples is lower than that reported for thermal sintering[4] mainly due to the considerably lower electrical conductivity. Further optimization of both the sintering parameter (e.g., using multiple pulses) and the film condition (e.g., particle sizes, film thicknesses) is required to achieve uniform sintering across the entire film thickness with improved film densities.

Table 1. Intense pulsed light parameters for single pulse sintering.

Substrate	Pulse duration [ms]	Power density [KW m^{-2}]	Sample designation
Glass	0.5	1.37	S-0.5-1.37
Glass	1	1.37	S-1-1.37
Glass	1.5	1.37	S-1.5-1.37
Glass	2	1.37	S-2-1.37
Kapton	1.5	0.9	Sk-1.5-0.9

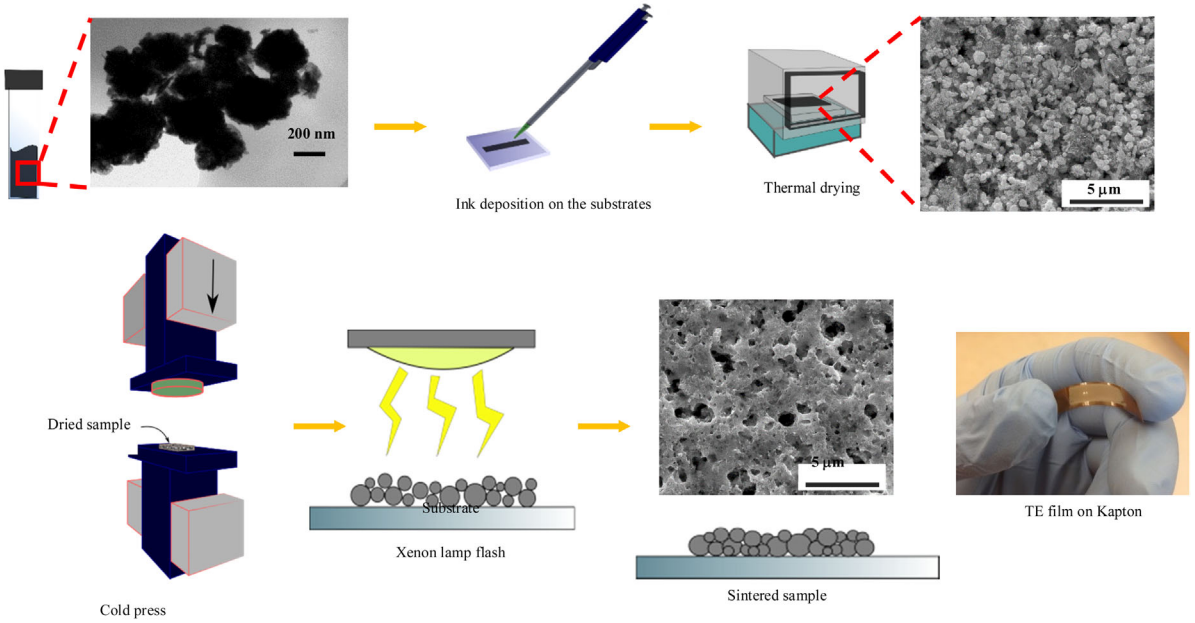

Figure 1. Schematic showing the TE film preparation by photonic sintering.

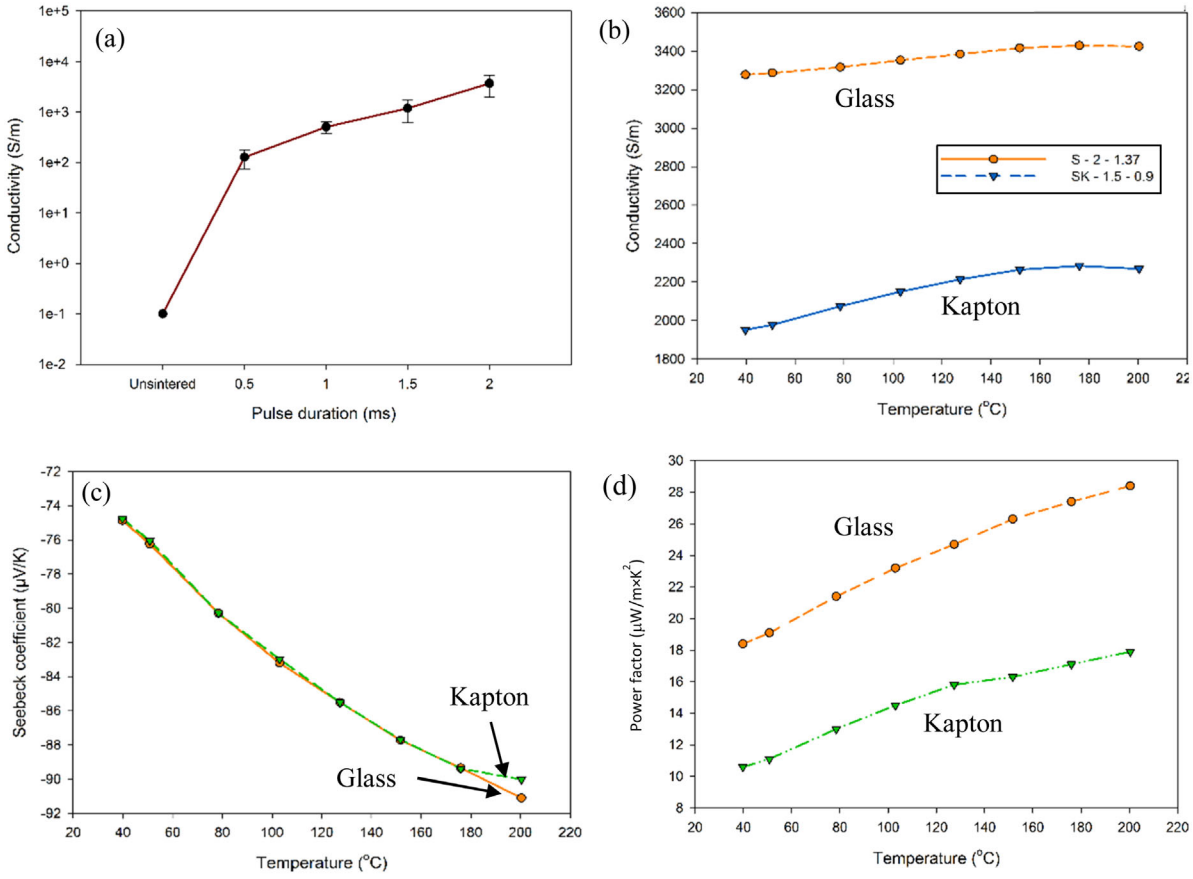

Figure 2. a) Electrical conductivity of the sintered samples by single pulse with increasing pulse duration from 0.5 to 2 milliseconds on glass. Temperature dependent (b) electrical conductivity (c) Seebeck coefficient (d) Power factor for the films on glass and Kapton substrate.

It is clear from the above results (Figure 2a–d) that the photonic flash can cause the TE nanoparticles to coalesce and sinter to form TE films. We can thus print the nanoparticles using any of the available printing methods (e.g., screen printing, inkjet printing, Aerosol Jet printing) onto any arbitrary flexible and/or rigid substrate followed by a photonic flash under ambient conditions to create TE films for various applications. The coalescence is achieved at a time scale of milliseconds (e.g., for single pulse samples) and thus is highly compatible with the rapid fabrication required for low cost manufacturing.

To gain an insight into the physical processes occurring during sintering, we modelled photonic sintering using COMSOL software as a thermo-plasmonic process[9] that selectively heats the nanoparticles, an approach similar to that used in the past by others.[7,10] Due to the length scales involved, this approach[7,10] divides the problem into finding the temperature rise in the top layer of the TE film due to the photonic flash, particle coalescence due to surface and volume diffusion triggered by temperature rises, and assessing the heat conduction into the rest of the film after the pulse has ended. Note that for the former, the model considers individual nanoparticles, while for the latter, the model assumes a film with length scales in micrometers. To maintain modeling practicality and estimate the temperature rise due to the photonic flash, we took a nanoparticle ensemble of 3×3 particles representing the top layer as shown in **Figure 3**a. The boundary conditions are similar that of a previous work.[7,10] The Figure 3a shows a system of 9 spherical nanoparticles in a 3×3 array to calculate the photonic heating and represent the "Top Layer" in Figure 3c. The film surface in Figure 3a is along the y-z plane. The electromagnetic wave of the flash propagates in the $-x$ direction in Figure 3a, while the electric field, E, is along the z direction. Only the right side of the three-particle layer are considered due to symmetry. The relevant parameters of the coalesced particles are shown in Figure 3b. The inter-particle neck growth and coalescence are based on mass transport by surface and grain boundary diffusion.[11]

The temperature rise of the nanoparticles as a result of the heat generation is shown in Figure 3d. For pulse durations of 0.5, 1, 1.5, and 2 ms, the temperature was calculated at time steps of 0.25, 0.5, 0.75, and 1 ms, respectively, until a time of 200 ms. The maximum temperature reached is about 780 K (507 °C) for the pulse with 2 ms duration. Note that the thermal sintering of these nanoparticles can be carried out at about 400–450 °C,[4] which indicates that photonic sintering can provide sufficient temperature within short time durations to cause particle coalescence. The maximum average temperature for 0.5 ms in Figure 3d is actually slightly lower than the thermal drying temperature prior to sintering. We note, however, that the intense pulsed light sintering process is a local heating process

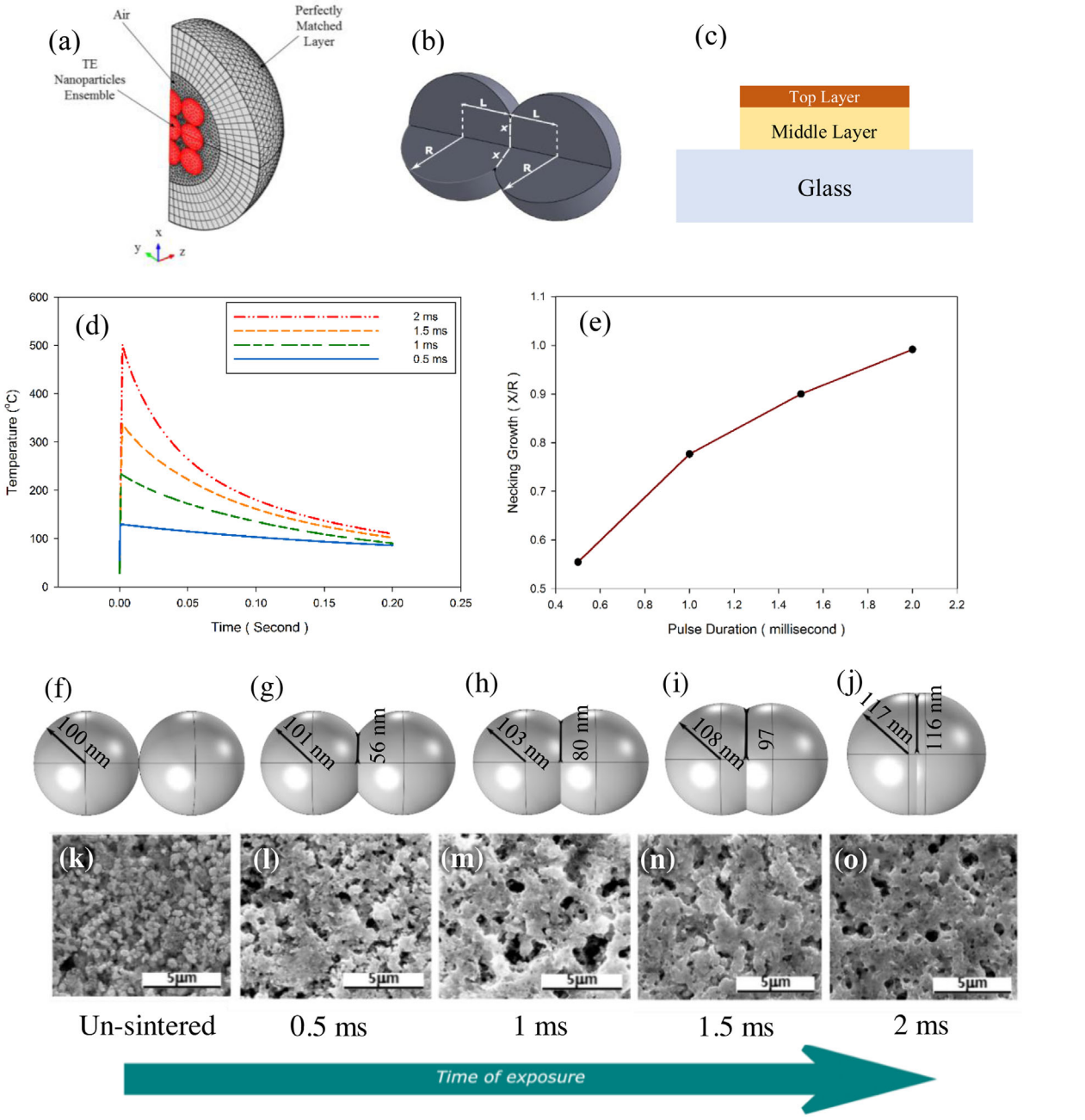

Figure 3. Model for the photonic sintering process of TE nanoparticles studied in this paper along with SEM images of the film under different photonic sintering conditions. a) Geometry of the top layer undergoing heating due to the photonic flash. b) Schematic of particle coalescence. c) 2D micro-scale geometry used to model the temperature profile of the middle layer. d) Temperature evolution captured by COMSOL's 'heat transfer in solid' module among top layers of particles. e) The necking growth represented by x/R for a pulse duration 0.5, 1, 1.5, and 2 ms pulse durations (conditions used for Figure 2*a*). f–j) Particle coalescence calculated by the model described in the paper. f) unsintered particles (g) sintered by 0.5 ms pulse duration (h) 1 ms, (i) 1.5 ms, and (j) 2 ms with fixed power density at 1.37 kW cm^{-2}. SEM images of the samples (k–o) sintered with 0 ms (unsintered), 1 ms, 1.5 ms, and 2 ms pulse duration. The model predictions (f–j) show good qualitative agreement with with the SEM images (k–o) for the film.

and at certain regions (e.g., particle contact points) the local temperature can exceed the average temperature to allow actual coalescence to take place. The coalescence of the particles as given by the ratio between the neck length and particle radius x/R, which varies from 0 to 1 (Figure 3b) for separated and fully coalesced particles, respectively. As shown in Figure 3e, the necking is seen to flatten out as a function of the pulse duration. This trend is not surprising, since at high x/R, a decrease in particle curvature results in a reduction in the chemical potential that drives the surface diffusion.[12]

The necking growth predicted in Figure 3e is shown pictorially in Figure 3f–j for the un-sintered sample and those

sintered with pulse durations of 0.5, 1, 1.5, and 2 ms, respectively. As the pulse time increases, more coalescence is observed from corresponding SEM images in Figure 3k–o. We see a qualitative agreement between the predicted particle coalescence and the SEM images. The porosity estimated for the Figure 3k–o is about 32%, 25%, 20%, 17%, and 16%, respectively. It is interesting to know that although the modeling predictions in Figure 3e show a diminishing return on the sintering process, the conductivity was seen to significantly increase in Figure 2a between the pulse durations of 1.5–2 ms. It is possible that the conductivity increases rapidly between 0.5 and 2 ms pulse duration due to increasing densification but may show a diminishing rise at pulse durations beyond 2 ms. Due to equipment limitations, it was not possible to investigate the coalescence behavior beyond the pulse duration of 2 ms.

It is clear from the above results that the pulsed light can sinter TE nanoparticles under ambient conditions to create continuous TE films. The photonic sintering process occurs at a time scale of milliseconds for single pulse sintering and a couple of seconds for multiple pulse sintering, which is several orders of magnitudes lower than that required for thermal sintering. Since the nanoparticles are locally heated during photonic sintering, the TE films could be fabricated on a flexible substrate such as Kapton which is very attractive for wearable and flexible energy harvesting devices. Further, the model used to predict the photonic heating gives important guidelines in selecting parameters influencing the TE film formation. The model predictions are shown to agree qualitatively with the SEM observations and the increase in conductivity.

We note that the degree of sintering observed in this work as reflected by the electrical conductivity is still an order of magnitude lower than that obtained under thermal sintering in vacuum.[4] Clearly, further optimization is necessary to increase the conductivity to match with that obtained by thermal sintering. In spite of these limitations, the first demonstration of the photonic sintering presented in this research can have a transformative effect on thermoelectric energy harvesting by printing and sintering nanoparticle films at arbitrary locations under ambient conditions without the need for complicated processes such as vacuum deposition or vacuum sintering.

In conclusion, we report the first demonstration of photonic sintering of TE nanoparticles to create functional TE films. An electrical conductivity of up to 3200 S m^{-1} is obtained for the films, representing an increase of about 5–6 orders of magnitude compared to compacted nanoparticles prior to sintering. This result shows promises of highly efficient, scalable and low-cost method to transform high-efficiency TE nanoparticles to economically viable thermoelectric devices for a wide variety of applications.

1. Experimental Section

TE Sample Preparation: During sample preparation, the TE nanoparticles were mixed with ethylene glycol (particle loading of 7 wt%) and sonicated for 10 min at 35 °C. The mixture was stirred for 24 h to create the dispersion of the TE nanoparticles in the solvent, that is, the nanoparticle ink. To prevent any further particle agglomeration, the ink was placed in a tube which was rotated continuously around its axis for at least 12 h using a tube roller (Scilogex MX-T6-S, Rocky Hill, CT) prior to dispensing on a substrate. Silica glass and flexible Kapton film[13] were used as substrates. The substrate surfaces were cleaned using an atmospheric O_2 plasma (AtomfloTM 400, Surfx Technologies LLC, Redondo Beach, CA) at 100 W power for 1 min to increase their hydrophilicity. The TE nanoparticles were dispensed on the substrates using a micro-pipette (HUAWEI, H200, Shenzhen, China) with 7 microliter volume. The as-prepared thin films had a thickness of 12–15 μm as measured by a profilometer (DekTak-XT, Bruker Instruments, San Jose, CA). The film thickness could be controlled by ink volume in the dispense area (10×3 mm^2). The film was dried in air at 150 °C for 30 min to partially remove the binders and solvents. A low ramp rate of 2 °C min^{-1} was used for this process to avoid any cracking in the film. The films were then cold compacted at a pressure of about 10 MPa in a universal testing machine (Instron Inc, Norwood, MA).

Flash Sintering of TE Nanoparticle Films: Once the films of the nanoparticles were cold compacted, a Sinteron 2000 flash lamp (Xenon Corp., USA) was used for photonic sintering of the dried films (Figure 1). The available pulse durations were 0.5, 1, 1.5, and 2 ms, with the sintering carried out in an ambient environment. The wavelength of the Xenon lamp ranged from 200 to 800 nm, with high intensity for wavelengths of 400–500 nm. The films were placed close to the focal point, that is, about 1 inch from the lamp. The morphology of the samples pre and post photonic sintering were examined through imaging using a scanning electron microscope (SEM, FEI Quanta 200F operating at 20 KV). Figure S1a–c show the representative TE film thickness profiles for samples after drying, after dry press, and after single pulse IPL sintering, respectively. The dried film thickness was about 12–15 um, which was reduced to about 5 um after cold press, indicating significant compaction. Upon exposure to photonic flash, the compacted film thickness was reduced to about 3.5 um, again indicating densification due to coalescence of the nanoparticles. The sintered films were also characterized by measuring their temperature dependent electrical conductivity and Seebeck coefficient. These measurements were done using a commercial Linsesis Seebeck and resistivity measurement apparatus with measurement error estimated to be about 2%.

Acknowledgements

The authors thank the Franceschi Microscopy Center at the Washington State University, Pullman for help with the SEM images for the work. Courtney Hollar was supported by the National Science Foundation Graduate Research Fellowship Program under Grant No. 1545659.

Supporting Information

Supporting Information is available from Wiley Online Library or from the author.

Conflict of Interest

The authors declare no conflict of interest.

Keywords

Bi-Te nanoparticles, energy harvesting, photonic sintering, power factor, thermoelectrics, ZT factor

Final Version: September 28, 2018
Received: July 20, 2018
Published online:

[1] a) D. M. Rowe, *CRC Handbook of Thermoelectrics*, CRC Press, Boca Raton, FL USA **1995**; b) I. Chowdhury, R. Prasher, K. Lofgreen, G. Chrysler, S. Narasimhan, R. Mahajan, D. Koester, R. Alley, R. Venkatasubramanian, *Nat. Nanotechnol*. **2009**, *4*, 235.
[2] L. E. Bell, *Science* **2008**, *321*, 1457.
[3] R. J. Mehta, Y. Zhang, C. Karthik, B. Singh, R. W. Siegel, T. Borca-Tasciuc, G. Ramanath, *Nat. Mater.* **2012**, *11*, 233.
[4] T. Varghese, C. Hollar, J. Richardson, N. Kempf, C. Han, P. Gamarachchi, D. Estrada, R. J. Mehta, Y. Zhang, *Sci. Rep*. **2016**, *6*, 33135.
[5] K. Hwang, Y. S. Jung, Y. J. Heo, F. H. Scholes, S. E. Watkins, J. Subbiah, D. J. Jones, D. Y. Kim, D. Vak, *Adv. Mater.* **2015**, *27*, 1241.
[6] a) G. L. Draper, R. Dharmadasa, M. E. Staats, B. W. Lavery, T. Druffel, *ACS Appl. Mater. Interfaces* **2015**, *7*, 16478; b) B. W. Lavery, S. Kumari, H. Konermann, G. L. Draper, J. Spurgeon, T. Druffel, *ACS Appl. Mater. Interfaces* **2016**, *8*, 8419; c) E. B. Secor, B. Y. Ahn, T. Z. Gao, J. A. Lewis, M. C. Hersam, *Adv. Mater.* **2015**, *27*, 6683.
[7] W. MacNeill, C.-H. Choi, C.-H. Chang, R. Malhotra, *Sci. Rep*. **2015**, *5*, 14845.
[8] a) D. Madan, Z. Wang, A. Chen, R.-C. Juang, J. Keist, P. K. Wright, J. W. Evans, *ACS Appl. Mater. Interfaces* **2012**, *4*, 6117; b) C. Navone, M. Soulier, M. Plissonnier, A. Seiler, *J. Electron. Mater.* **2010**, *39*, 1755; c) J. H. We, S. J. Kim, G. S. Kim, B. J. Cho, *J. Alloys Compd*. **2013**, *552*, 107.
[9] a) A. O. Govorov, W. Zhang, T. Skeini, H. Richardson, J. Lee, N. A. Kotov, *Nanoscale Res. Lett*. **2006**, *1*, 84; b) X. Zheng, H. Lee, T. H. Weisgraber, M. Shusteff, J. DeOtte, E. B. Duoss, J. D. Kuntz, M. M. Biener, Q. Ge, J. A. Jackson, S. O. Kucheyev, N. X. Fang, C. M. Spadaccini, *Science* **2014**, *344*, 1373; c) K. L. Kelly, E. Coronado, L. L. Zhao, G. C. Schatz, *J. Phys. Chem. B* **2003**, *107*, 668.
[10] S. Bansal, R. Malhotra, *Nanotechnology* **2016**, *27*, 495602.
[11] F. Parhami, R. McMeeking, A. Cocks, Z. Suo, *Mech. Mater.* **1999**, *31*, 43.
[12] P. Shewmon, *Diffusion in Solids*, Springer, Basel, Switzerland **2016**.

